Local electronic signatures of impurity states in graphene

T. O. Wehling,[1] A. V. Balatsky,[2,*] M. I. Katsnelson,[3] A. I. Lichtenstein,[1] K. Scharnberg,[1] and R. Wiesendanger[4]
[1]*I. Institut für Theoretische Physik, Universität Hamburg, Jungiusstraße 9, D-20355 Hamburg, Germany*
[2]*Theoretical Division, Los Alamos National Laboratory, Los Alamos, New Mexico 87545, USA*
[3]*Institute for Molecules and Materials, University of Nijmegen, Toernooiveld 1, 6525 ED Nijmegen, The Netherlands*
[4]*I. Institut für Angewandte Physik, Universität Hamburg, Jungiusstraße 11, D-20355 Hamburg, Germany*
(Received 1 February 2007; published 26 March 2007)

Defects in graphene are of crucial importance for its electronic and magnetic properties. Here, impurity effects on the electronic structure of surrounding carbon atoms are considered and the distribution of the local densities of states is calculated. As the full range from near field to the asymptotic regime is covered, our results are directly accessible by scanning tunneling microscopy. We also include exchange scattering at magnetic impurities and elucidate how strongly spin-polarized impurity states arise.

DOI: 10.1103/PhysRevB.75.125425 PACS number(s): 81.05.Uw, 68.37.Ef, 71.55.−i, 71.15.Mb

I. INTRODUCTION

Graphene, a recently discovered allotrope of carbon and the first known example of a truly two-dimensional (2D) crystal,[1,2] has unique electronic properties,[3–17] such as an exotic quantum Hall effect with half-integer quantization of the Hall conductivity,[3,4] finite conductivity at zero charge-carrier concentration,[3] strong suppression of weak localization,[13] etc. The peculiar 2D band structure of graphene resembles ultrarelativistic electron dynamics near two nodal points in the Brillouin zone. This provides a new bridge between condensed matter theory and quantum electrodynamics (index theorem and the half-integer quantum Hall effect,[3] relativistic Zitterbewegung[18] and the minimal conductivity,[12] and "Klein paradox"[19] and anomalous tunneling of electrons in graphene through potential barriers[16]). Unexpectedly, high electron mobility in graphene and its perfect suitability for planar technology make it a prospective material for next-generation, carbon-based electronics.[1]

Impurity states are important contributors to these unusual properties. Graphene is conducting due to carriers that can be introduced either by a gate voltage[1,3,4] or by doping.[1,8,9] This situation is very reminiscent of doped semiconductors, where the desired properties are obtained by creating an impurity band. Recent progress in scanning tunneling microscopy (STM) made it possible to image impurity states for a wide class of materials with very high spatial resolution. This so-called "wave-function imaging" yields local images of the impurity-induced wave function. Examples of wave function imaging range from unconventional superconductors[20,21] to semiconductors,[22,23] magnetic metals,[24] and graphite surfaces.[25–28] It allows one to investigate the formation of the impurity band and the associated electronic properties. Theoretical modeling and STM measurements of near impurity site effects can be compared and thus elucidate, e.g., magnetic interaction mechanisms.[23,29]

The purpose of this paper is to address the question of electronic properties of single and double impurities in graphene in connection with future STM experiments and impurity-induced ferromagnetism. The impurity states are characterized by their energy and by their real-space wave functions that determine the shape of the resonance. In contrast to previous studies,[9,10,15] we consider the real-space structure of the electronic state in the range from the impurity site to the asymptotic regime, its dependence on the potential strength, and the spin-exchange interaction.

The honeycomb arrangement of carbon atoms in graphene can be described by a hexagonal lattice with two sublattices A and B (see, e.g., Ref. 30). With the Fermi operators c_i and d_i of electrons in cell i at sublattices A and B, respectively, we describe a single and two neighboring impurities by $V_s = U_0 c_0^\dagger c_0$ and $V_d = U_0(c_0^\dagger c_0 + d_0^\dagger d_0) + U_1(c_0^\dagger d_0 + d_0^\dagger c_0)$. Here, U_0 is the potential strength and U_1 the change of sublattice hopping between the two impurity sites. Related to the current research are questions about impurities in graphite that have been studied with STM.[25–28] Only the atoms above hollow sites are seen in STM on graphite. We find that impurity states in graphene are *qualitatively* different from those in graphite because of the sublattice degeneracy that is reflected in a complicated sublattice structure of impurity-induced resonances.

We find that impurity scattering produces low-energy resonances with the real-space structure and the resonant energy E_{imp} as a function of U_0 (and U_1) clearly distinguishes between single and double impurities. For single impurities, we find in agreement with Skrypnyk and Loktev[11] that E_{imp} is well described by

$$U_0 = \frac{W^2}{E_{\mathrm{imp}} \ln \left| \frac{E_{\mathrm{imp}}^2}{W^2 - E_{\mathrm{imp}}^2} \right|}, \tag{1}$$

where W is the bandwidth. Hence, the resonance energy E_{imp} approaches zero for $U_0 \to \infty$. Only strong single impurities (i.e., $U_0 \gtrsim 10$ eV) are capable of producing resonances within 1 eV of the Dirac point. This result is similar to the impurity states observed in unconventional superconductors with Dirac spectrum.[31]

The resonance of a double impurity is basically determined by $U_0 - U_1$. Its energy coincides with the Dirac point at *finite* $U_0 - U_1 = 3t$, where $t \approx 2.7$ eV is the nearest-neighbor hopping parameter of graphene.

We give a detailed description of the local density of states (LDOS), the real-space fingerprint of impurities in

 ©2007 The American Physical Society

graphene. Near the impurity site that LDOS exhibits an intricate pattern. A single strong impurity placed on one sublattice produces a peak in LDOS at low energies that is large on the other sublattice. At large distances, these impurity resonances have wave functions ψ that asymptotically decay as $|\psi|^2 \propto 1/r$.

We will consider potential scattering (nonmagnetic) as well as magnetic impurities, i.e., spin-dependent scattering. In the latter case, the impurity-induced resonance will exhibit a spin-dependent splitting that might lead to a strong spin polarization of the impurity state. This observation, we believe, is important for the discussion of moment formation and possible magnetic order in graphene.

II. MODEL AND RESONANT ENERGIES OF THE IMPURITY STATES

To start with our *theoretical model*, we describe the carbon p_z electrons within the tight-binding approximation by $H=\int_{\Omega_B}\frac{d^2k}{\Omega_B}\Psi^\dagger(k)H_k\Psi(k)$ with

$$\Psi(k)=\begin{bmatrix} c(k) \\ d(k) \end{bmatrix}$$

and

$$H_k=\begin{pmatrix} 0 & \xi(k) \\ \xi^*(k) & 0 \end{pmatrix},$$

where $\xi(k)=t\Sigma_{j=1}^{3}e^{ik(b_j-b_1)}$. Ω_B denotes the Brillouin zone volume and $c(k)$ $[d(k)]$ are the k-space counterparts of c_i (d_i).[30]

The full Green's function in real space $G(i,j,E)$ will be obtained using the T matrix formalism,

$$G(i,j,E)=G^0(i-j,E)+G^0(i,E)T(E)G^0(-j,E). \quad (2)$$

Therefore, the unperturbed Green's function $G^0(i,E)$ in real space is calculated from its k-space counterpart $\tilde{G}^0(k,E)=(E-H_k+i\delta)^{-1}$ by Fourier transformation. Numerical problems in carrying out the Fourier integrals are avoided by linearizing the band structure in a vicinity of the Dirac points, where all singularities occur. Outside these regions, the full tight-binding band structure is taken into account. Finally, the T matrix is given by $T(E)=[\mathbf{1}-\tilde{V}_{s(d)}G^0(0,E)]^{-1}\tilde{V}_{s(d)}$ with

$$\tilde{V}_s=U_0\begin{pmatrix} 1 & 0 \\ 0 & 0 \end{pmatrix}$$

and

$$\tilde{V}_d=\begin{pmatrix} U_0 & U_1 \\ U_1 & U_0 \end{pmatrix}$$

being the impurity potentials in k-space and matrix form. Poles of the T matrix corresponding to impurity resonances occur, if $\det[\mathbf{1}-\tilde{V}_{s,d}G^0(0,E)]=0$, i.e.,

$$U_0G_{11}^0(0,E)-1=0 \quad (3)$$

for a single scatterer and

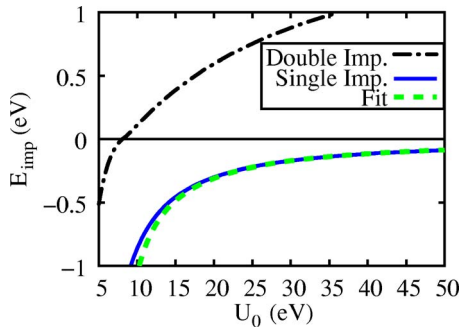

FIG. 1. (Color online) The energy E_{imp} of the impurity resonance as a function of the potential strength U_0 is shown for single impurities and double impurities with $U_1=0$. For the single scatterer, E_{imp} obtained from our tight-binding calculation is compared to the result obtained from the fully linearized band structure [Eq. (1)] with fitted bandwidth $W=6.06$ eV.

$$[1-U_0G_{11}^0(0,E)]^2-U_0^2G_{21}^0(0,E)G_{12}^0(0,E)=0 \quad (4)$$

for double impurity with $U_1=0$—this case, we refer to as scalar impurity. Equations (3) and (4) have solutions corresponding to attractive and repulsive potentials U_0. We limit our discussion to the latter case, as the former is obtained by reversing the signs of all energies. Near the Dirac points, we have $|\text{Re}(G^0)| \gg |\text{Im}(G^0)|$ so that the impurity resonances E_{imp} as function of U_0 can be calculated from the previous two equations considering only the $\text{Re}(G^0)$: The resulting real *impurity energies* as a function of U_0 are shown in Fig. 1. Adjusting the bandwidth parameter W in Eq. (1) to fit our $E_{\text{imp}}(U_0)$ yields $W=6.06\pm0.02$ eV. An estimation of W can be obtained by assuming linear dispersion in the entire Brillouin zone: $W=\hbar v_f k_c$, where k_c is the cutoff wave number. Approximating the Brillouin zone by two circles with radius k_c around the two nonequivalent Dirac points results in $\Omega_B=2\pi k_c^2$ and correspondingly $W=\hbar v_f\sqrt{\frac{\Omega_B}{2\pi}}\approx 6.3$ eV. That is, the estimated and the fitted bandwidth differ only slightly.

It is quite remarkable that a pair of neighboring scatterers produces a resonance at the Dirac point for $U_0=3t\approx 8.1$ eV, while for a single impurity this occurs only in the limit of infinite potential strength. This effect can be attributed to the existence of *two* nonequivalent Dirac points in the Brillouin zone. As a consequence, at $E=0$ the on-site Green's function $G^0(0,0)$ has finite off-diagonal $G_{12}^0(0,0)=G_{21}^0(0,0)=-\frac{1}{3t}$ but vanishing diagonal components resulting via Eqs. (3) and (4) in the characteristic $E_{\text{imp}}(U_0)$ curves.

For double impurities with sublattice hopping change U_1, it follows directly from the secular equation that the impurity energy as a function of U_0 and U_1 is obtained from the scalar case by replacing U_0 with U_0-U_1.

III. REAL-SPACE IMAGE OF THE IMPURITY STATES

We obtained the LDOS $N(r,E)=-\frac{1}{\pi}\text{Im}[\Sigma_{i,j}\Phi_i(r)G(i,j,E)\Phi_j^\dagger(r)]$ in the presence of impurities as a function of position and energy, where $\Phi_i(r)=[\phi_i^c(r),\phi_i^d(r)]$ with $\phi_i^{c,d}(r)$ being carbon p_z orbitals located in the unit cell i at sublattices A and B, respectively. This LDOS of impurity reso-

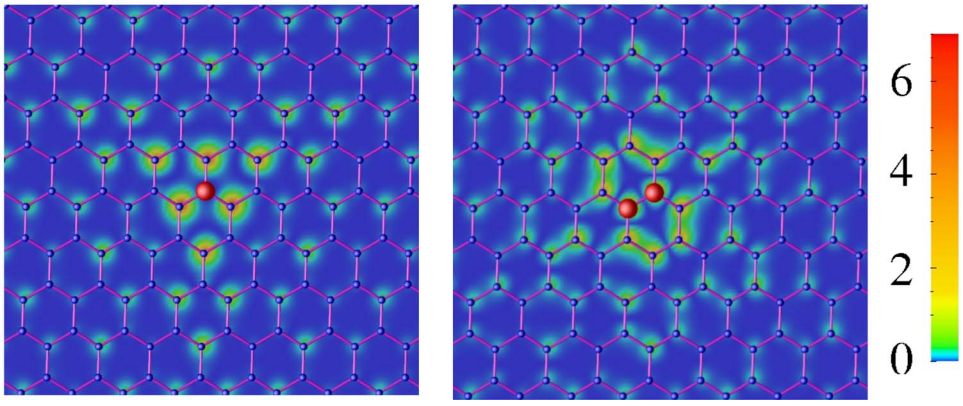

FIG. 2. (Color online) r-dependent LDOS at $E=E_{\mathrm{imp}}=-0.1$ eV for a single impurity with $U_0=45$ eV (left) and for a scalar double impurity with $U_0=6.9$ eV (right) encoded corresponding to color bar. The impurity sites are marked as big dots in the center of the images.

nances at $E_{\mathrm{imp}}=-0.1$ eV for single and scalar impurities are shown in Fig. 2.[32] The formation of virtual bound states (VBSs) due to impurity scattering is clearly visible.

These VBSs are a general feature of localized states hybridizing with a continuum of delocalized states. They have been observed in many systems ranging from elementary metals[33] to d-wave superconductors.[31] Details of the real-space image are, however, system specific. Here, the threefold (D_{3h}) symmetry of the VBS for a single impurity and twofold (D_{2h}) symmetry for a double impurity are direct consequences of the lattice symmetry. The (D_{3h}) symmetric single impurity state results in sixfold symmetric Fourier-transformed scanning tunneling spectra.[34] Furthermore, the peculiarities of the band structure of graphene manifest themselves in the near-field characteristics of impurities: A single impurity in sublattice A induces an impurity state mostly localized in sublattice B and vice versa due to the fact that $G^0_{11}(i,E) \ll G^0_{12}(i,E), G^0_{21}(i,E)$ for $E \to 0$, which can be attributed to the existence of two nonequivalent Dirac points as explained above.

The site projected DOS $N(i,E)$ can be obtained from the full Green's function $N(i,E)=-1/\pi \,\mathrm{Im}\, G(i,i,E)$, where each of the diagonal matrix elements corresponds to one sublattice. For the single impurity and U_0 from 10 to 40 eV, the LDOS at the impurity, nearest-neighbor (NN), and next-NN sites are shown in Fig. 3. One sees that for vacancies with $10 \lesssim U_0 \lesssim 20$ eV,[8] but not for weaker potentials, an impurity resonance should be clearly observable within 1 eV around the Dirac point.

It further illustrates the localization of the impurity state on sublattice B, when the impurity is in sublattice A, as well as the reduction of LDOS at the impurity site for strong repulsive potential. The LDOS at the impurity site in Fig. 3 (left) is in agreement with Ref. 11, where a similar model has been applied. The double impurity respects pseudospin symmetry and is much more sensitive to weaker potentials, as obvious from Fig. 4. Clearly, $U_t=U_0-U_1$ is the most important parameter determining the shape of LDOS in the case of a double impurity: The results for ($U_0=4$ eV and $U_1=-2$ eV) and ($U_0=6$ eV and $U_1=0$ eV) are virtually indistinguishable at the impurity resonance but differ slightly below it. For large distances $r \gg \hbar v_f/E_{\mathrm{imp}}$ from the impurity site, we obtain for the changes in LDOS $\Delta N(r,E_{\mathrm{imp}}) \propto 1/r$ in agreement with Refs. 34 and 35 for all considered types of impurities. Note the contrast to a single hard-wall impurity, i.e., $U_0 \to \infty$, with $1/r^2$ asymptotics of $\Delta N(r,E_{\mathrm{imp}})$.[7]

IV. MAGNETIC IMPURITIES

If the impurities have a *magnetic moment*, exchange scattering of the graphene p_z electrons and the spin S localized at the impurity site will occur. As long as the exchange coupling J does not exceed a critical value, Kondo screening of the spin S by the band electrons can be neglected and the impurity spin acts as local magnetic field: The effective scattering potential is renormalized to $U_0 \pm J$. The resulting change in spin-polarized (SP) LDOS in the vicinity of a single impurity is shown in Fig. 5 for $U_0=12$ eV and J

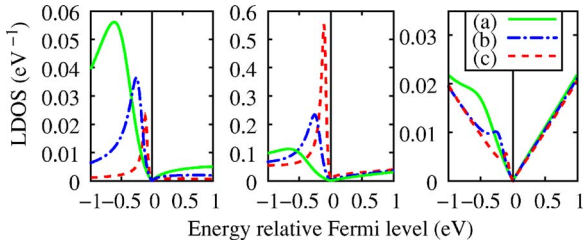

FIG. 3. (Color online) LDOSs at the impurity site (left), NN site (middle), and NNN site (right) are shown for a single impurity with potentials U_0=(a) 10 eV, (b) 20 eV, and (c) 40 eV.

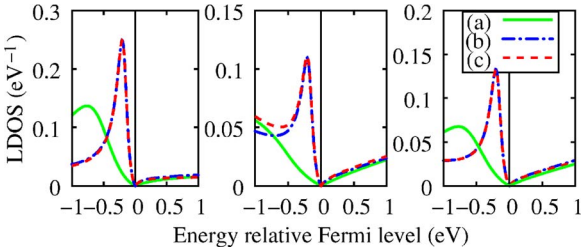

FIG. 4. (Color online) As in Fig. 3 but for scalar double impurity with U_0=(a) 4 eV and (c) 6 eV as well as for double impurity with $U_0=4$ eV and U_1=(b) −2 eV.

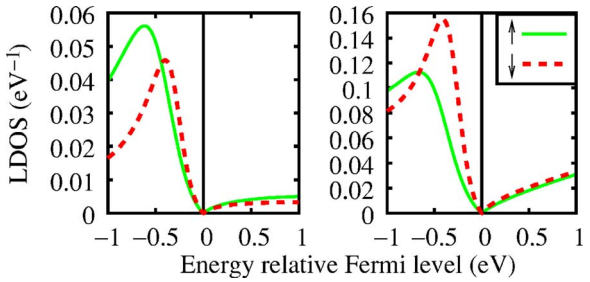

FIG. 5. (Color online) SP-LDOSs at the impurity site (left) and a NN site (right) are shown for a single magnetic impurity with $U_0=12$ eV and $J=2$ eV.

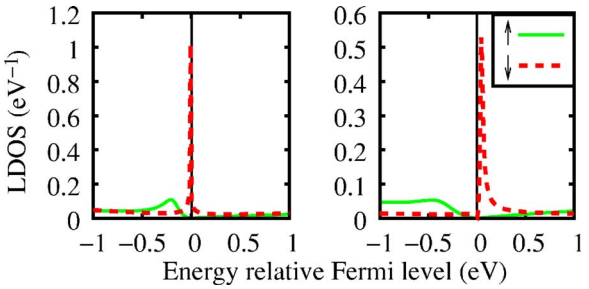

FIG. 6. (Color online) SP-LDOSs at a NN site of a double impurity with $U_0=5$ eV, $U_1=-2$ eV, and $J=1$ eV (left) and 2 eV (right) are shown.

=2 eV. The exchange splitting of the resonances in the two spin channels is approximately 0.15 eV. This type of exchange scattering also affects decay lengths and oscillation periods of the induced spin-density variations and therefore provides a possible mechanism for long-range exchange interactions.

For double impurities, the effect of exchange splitting is much more pronounced within a realistic parameter range: As Fig. 6 shows, exchange scattering can produce strongly spin-polarized impurity states. The impurity resonances of one spin channel can be pushed close to the Dirac point, or the impurity levels are split even below and above it.

Depending on the type of impurities, the spin polarization of the impurity states can strongly depend on doping: In the example with $J=2$ eV, the VBS above the Dirac point can be occupied by spin-down electrons due to n doping.

It was demonstrated recently[36] that ferromagnetism of *sp* electrons in narrow impurity bands can be characterized by much higher Curie temperatures than those typical for traditional dilute magnetic semiconductors. Hence, the impurity band associated with the magnetic impurities considered in this paper can be a promising candidate for facilitating high-temperature ferromagnetic order in graphene.

V. CONCLUSIONS AND OUTLOOK

We have calculated the LDOS of impurity resonances in graphene from the near field to the regime of asymptotic $1/r$ decay. The near-field LDOSs are directly observable by STM and comparison of upcoming experiments with our predictions will elucidate the nature of impurities in graphene. We also find that impurity resonances in graphene are very different from the impurity states observed in graphite because of the two sublattice structure in graphene.

We showed further how spin-polarized impurity states can result from exchange scattering at magnetic impurities and their sensitivity to doping. The resulting formation of spin polarized impurity bands may give rise to long-range exchange interactions and magnetic order that can be directly studied by spin-polarized STM.

ACKNOWLEDGMENTS

We are grateful to M. Bode, A. Castro Neto, J. Fransson, A. Geim, A. Kubetzka, K. Novoselov, and J. X. Zhu for useful discussions. This work has been supported by LDRD and DOE BES at Los Alamos, FOM (Netherlands), and SFB 668. A.V.B. is grateful to U. Hamburg and Wiesendanger group for hospitality during the visit, when the ideas presented in this work were conceived.

*Electronic address: avb@lanl.gov; URL: http://theory.lanl.gov

[1] K. S. Novoselov, A. K. Geim, S. V. Morozov, D. Jiang, Y. Zhang, S. V. Dubonos, I. V. Grigorieva, and A. A. Firsov, Science **306**, 666 (2004).

[2] K. S. Novoselov, D. Jiang, F. Schedin, T. J. Booth, V. V. Khotkevich, S. V. Morozov, and A. K. Geim, Proc. Natl. Acad. Sci. U.S.A. **102**, 10451 (2005).

[3] K. S. Novoselov, A. K. Geim, S. V. Morozov, D. Jiang, M. I. Katsnelson, I. V. Grigorieva, S. V. Dubonos, and A. A. Firsov, Nature (London) **438**, 197 (2005).

[4] Y. Zhang, Y.-W. Tan, H. L. Stormer, and P. Kim, Nature (London) **438**, 201 (2005).

[5] M. A. H. Vozmediano, M. P. Lopez-Sancho, T. Stauber, and F. Guinea, Phys. Rev. B **72**, 155121 (2005).

[6] N. M. R. Peres, F. Guinea, and A. H. Castro Neto, Phys. Rev. B **72**, 174406 (2005).

[7] V. M. Pereira, F. Guinea, J. M. B. Lopes dos Santos, N. M. R. Peres, and A. H. Castro Neto, Phys. Rev. Lett. **96**, 036801 (2006).

[8] See Y. G. Pogorelov, cond-mat/0603327 (unpublished). Using density functional theory we obtain similar estimations, e.g., $U_0\approx 18$ eV for vacancies.

[9] N. M. R. Peres, F. Guinea, and A. H. Castro Neto, Phys. Rev. B **73**, 125411 (2006).

[10] H. Kumazaki and D. S. Hirashima, J. Phys. Soc. Jpn. **75**, 053707 (2006).

[11] Y. V. Skrypnyk and V. M. Loktev, Phys. Rev. B **73**, 241402(R) (2006).

[12] M. I. Katsnelson, Eur. Phys. J. B **51**, 157 (2006).

[13] S. V. Morozov, K. S. Novoselov, M. I. Katsnelson, F. Schedin, L. A. Ponomarenko, D. Jiang, and A. K. Geim, Phys. Rev. Lett. **97**, 016801 (2006).

[14] V. V. Cheianov and V. I. Fal'ko, Phys. Rev. B **74**, 041403(R) (2006).
[15] V. V. Cheianov and V. I. Fal'ko, Phys. Rev. Lett. **97**, 226801 (2006).
[16] M. I. Katsnelson, K. S. Novoselov, and A. K. Geim, Nat. Phys. **2**, 620 (2006).
[17] T. C. Li and S.-P. Lu, cond-mat/0609009 (unpublished).
[18] Zitterbewegung means the uncertainty of the position of relativistic particles due to the creation of particle-antiparticle pairs, when attempting to localize a particle.
[19] Klein Paradox refers to the penetration of relativistic particles through arbitrarily wide potential barriers, if the potential is sufficiently high (see more in Ref. 16).
[20] S. H. Pan, E. W. Hudson, K. M. Lang, H. Eisaki, S. Uchida, and J. C. Davis, Nature (London) **403**, 746 (2000).
[21] E. W. Hudson, K. M. Lang, V. Madhavan, S. H. Pan, H. Eisaki, S. Uchida, and J. C. Davis, Nature (London) **411**, 920 (2001).
[22] T. Maltezopoulos, A. Bolz, C. Meyer, C. Heyn, W. Hansen, M. Morgenstern, and R. Wiesendanger, Phys. Rev. Lett. **91**, 196804 (2003).
[23] D. Kitchen, A. Richardella, J.-M. Tang, M. E. Flatte, and A. Yazdani, Nature (London) **442**, 436 (2006).
[24] K. von Bergmann, M. Bode, A. Kubetzka, M. Heide, S. Blügel, and R. Wiesendanger, Phys. Rev. Lett. **92**, 046801 (2004).
[25] H. A. Mizes and J. S. Foster, Science **244**, 559 (1989).
[26] K. F. Kelly, D. Sarkar, G. D. Hale, S. J. Oldenburg, and N. J. Halas, Science **273**, 1371 (1996).
[27] K. F. Kelly, E. T. Mickelson, R. H. Hauge, J. L. Margrave, and N. J. Halas, Proc. Natl. Acad. Sci. U.S.A. **97**, 10318 (2000).
[28] T. Matsui, H. Kambara, Y. Niimi, K. Tagami, M. Tsukada, and H. Fukuyama, Phys. Rev. Lett. **94**, 226403 (2005).
[29] J.-M. Tang and M. E. Flatte, Phys. Rev. Lett. **92**, 047201 (2004).
[30] G. W. Semenoff, Phys. Rev. Lett. **53**, 2449 (1984).
[31] A. V. Balatsky, I. Vekhter, and J.-X. Zhu, Rev. Mod. Phys. **78**, 373 (2006).
[32] $E_{\mathrm{imp}}=-0.1$ eV requires $U_0=45$ eV for a single impurity. Being a fitting parameter for experiments, this choice of U_0 is made to illustrate the resonance near Dirac point.
[33] V. A. Gubanov, A. I. Liechtenstein, and A. V. Postnikov, *Magnetism and the Electronic Structure of Crystals* (Springer, Berlin, 1992).
[34] C. Bena and S. A. Kivelson, Phys. Rev. B **72**, 125432 (2005).
[35] D.-H. Lin, Phys. Rev. A **73**, 044701 (2006).
[36] D. M. Edwards and M. I. Katsnelson, J. Phys.: Condens. Matter **18**, 7209 (2006).